Applied Ergonomics

Bipolar versus High-Density surface electromyography for evaluating risk in fatiguing frequency-dependent lifting activities

--Manuscript Draft--

Manuscript Number:	
Article Type:	Full Length Article
Keywords:	Bipolar and High-Density (HD) sEMG; biomechanical risk; fatiguing frequency-dependent lifting activities
Corresponding Author:	TIWANA VARRECCHIA, Ph.D. ITALY
First Author:	Tiwana Varrecchia
Order of Authors:	Tiwana Varrecchia
	Alberto Ranavolo
	Silvia Conforto
	Alessandro Marco De Nunzio
	Michail Arvanitidis
	Francesco Draicchio
	Deborah Falla
Abstract:	This study aims to verify the hypothesis that the combined use of high-density surface electromyography (HDsEMG) and segmental kinematic assessment allows an optimized discrimination of risk levels associated with different fatigue lifting conditions. 15 participants performed three lifting tasks lasting 15 minutes (Lifting Index(LI): 1, 2 and 3). Kinematic of upper body and electromyographic data of erector spinae (ES) muscle were recorded using, respectively, Inertial Measurement Units (IMUs) and both electromyographic bipolar and HD systems. The ANOVA showed that each pair of LI can be significantly discriminated by the root mean square of the acceleration magnitude only for the IMU on the arm, of bipolar sEMG at last two minutes of the task and of HD grid starting from the 4 th minute. Additionally, the topographical maps of EMG amplitude show that the ES activity distribution changes between the beginning and the end of the session especially in the high-risk condition.
Suggested Reviewers:	Roberta Bonfiglioli roberta.bonfiglioli@unibo.it
	Pascal Max Madeleine pm@hst.aau.dk
	Antonio Gogeascoechea a.d.j.gogeascoecheahernandez@utwente.nl
	Kostas Nizamis k.nizamis@utwente.nl
	Guillaume Durandau g.v.durandau@utwente.nl

Rome 05/11/2020

Subject: Submission of a manuscript to “Applied Ergonomics”

Title: Bipolar versus High-Density surface electromyography for evaluating risk in fatiguing frequency-dependent lifting activities

Authors: Tiwana Varrecchia, Alberto Ranavolo, Silvia Conforto, Alessandro Marco De Nunzio, Michail Arvanitidis, Francesco Draicchio and Deborah Falla

Dear Editor,

Attached you will find the electronic version of the manuscript entitled “Bipolar versus High-Density surface electromyography for evaluating risk in fatiguing frequency-dependent lifting activities” which we would like to submit for publication in “Applied Ergonomics”. The manuscript deals with the quantitative assessment of fatiguing lifting tasks through the use of features extracted from Inertial Measurement Units, surface bipolar and High-Density EMG signals recorded from multiple trunk muscles.
We think that the manuscript could be of interest to a vast audience of readers of “Applied Ergonomics”. The manuscript has been prepared in accordance with the Instructions to authors of “Applied Ergonomics”. The manuscript has never been submitted elsewhere before, nor it is under consideration at other editorial offices.
This final draft of the manuscript has been approved by the listed authors, all of whom have made substantial contributions to the conception and design of the study, performing experiments, revising the article and approving the final version.

Thanks for your attention.

Kind Regards,
Tiwana Varrecchia

Department of Occupational and Environmental Medicine, Epidemiology and Hygiene, INAIL, Monte Porzio Catone, 00040 Rome, Italy; t.varrecchia@inail.it

Manuscript

Bipolar versus High-Density surface electromyography for evaluating risk in fatiguing frequency-dependent lifting activities

Tiwana Varrecchia [1,2], Alberto Ranavolo [1], Silvia Conforto [2], Alessandro Marco De Nunzio [3], Michail Arvanitidis [4], Francesco Draicchio [1] and Deborah Falla [4]

[1] Department of Occupational and Environmental Medicine, Epidemiology and Hygiene, INAIL, Monte Porzio Catone, 00040 Rome, Italy; t.varrecchia@inail.it (T.V.); a.ranavolo@inail.it (A.R.); f.draicchio@inail.it (F.D.)

[2] Department of Engineering, Roma Tre University, Via Vito Volterra 62, Roma, Lazio, Italy; silvia.conforto@uniroma3.it (S.C.)

[3] LUNEX International University of Health, Exercise and Sports, 50, Avenue du Parc des Sports, Differdange, 4671, Luxembourg; alessandro.denunzio@lunex-university.net (A.M.D.N.)

[4] Centre of Precision Rehabilitation for Spinal Pain (CPR Spine), School of Sport, Exercise and Rehabilitation Sciences, University of Birmingham, Edgbaston, B152TT, United Kingdom; MXA1016@student.bham.ac.uk (A.M.); D.Falla@bham.ac.uk (D.F.)

Corresponding author: t.varrecchia@inail.it

Abstract: This study aims to verify the hypothesis that the combined use of high-density surface electromyography (HDsEMG) and segmental kinematic assessment allows an optimized discrimination of risk levels associated with different fatigue lifting conditions. 15 participants performed three lifting tasks lasting 15 minutes (Lifting Index(LI): 1, 2 and 3). Kinematic of upper body and electromyographic data of erector spinae (ES) muscle were recorded using, respectively, Inertial Measurement Units (IMUs) and both electromyographic bipolar and HD systems. The ANOVA showed that each pair of LI can be significantly discriminated by the root mean square of the acceleration magnitude only for the IMU on the arm, of bipolar sEMG at last two minutes of the task and of HD grid starting from the 4th minute. Additionally, the topographical maps of EMG amplitude show that the ES activity distribution changes between the beginning and the end of the session especially in the high-risk condition.

Keywords: Bipolar and High-Density (HD) sEMG; biomechanical risk; fatiguing frequency-dependent lifting activities.

---

1. Introduction

To prevent the onset of work-related low-back disorders (WLBDs) related to the manual lifting of heavy loads and to evaluate the effectiveness of ergonomic interventions, it is crucial to perform an accurate biomechanical risk assessment. Among others, the Revised National Institute for Occupational Safety and Health (NIOSH) Lifting Equation (RNLE) (Waters et al., 1993, 1994) allows health and safety practitioners to assess manual lifting efforts, albeit with some drawbacks due to equation and parameter restrictions (Lavander et al., 2009).

In addition to RNLE, several promising instrumental-based assessment tools have been designed and developed in recent years (Alberto et al., 2018). These quantitative approaches rely on the computation of kinematic, kinetic and surface electromyography (sEMG)-based indices such as mechanical energy consumption (Ranavolo et al., 2017), compression and shear forces at the 5th lumbar and 1st sacral vertebra of the spine (Ranavolo et al., 2018a) and trunk muscle co-activation

(Ranavolo et al., 2018a, 2015). These indices are sensitive to different lifting risk conditions and are positively correlated to stress parameters on the sacral-lumbar region of the spine (i.e. compressive and shear forces in that region). These quantitative methods have significant advantages. They can be used in scenarios where RNLE cannot such as lifting while seated or kneeling, in a restricted workspace, unstable objects, while carrying, pushing, or pulling and in unfavorable environments. Furthermore, the computational cost for indices calculation is very low and the recording of signals from the human body can be achieved with unobtrusive, wireless, wearable, miniaturized and low power consumption sensors (Alberto et al., 2018). The most commonly used systems are inertial measurement units (IMUs), wireless shoe insoles for ground reaction force measurement and bipolar sEMG probes. Instrument-based tools for biomechanical risk classification can be optimized by the use of machine-learning techniques, such as artificial neural networks (ANNs), which have high performance when appropriate kinematic and sEMG datasets are selected (Varrecchia et al., 2018, 2020).

By contrast, the capacity of these approaches to detect the biomechanical risk is currently limited only to single frequency-independent lifting task (single repetition of task) (Waters et al., 1994) with no adjustments for the influence of muscle fatigue. Indeed, previous studies (Ranavolo et al., 2015, 2017, 2018a; Varrecchia et al., 2018, 2020) involved lifting tasks were designed to be executed at a lifting frequency ≤ 0.2 lift/min providing frequency multipliers of RNLE always equal to 1 (not affecting the RNLE). The use of sEMG-based biomechanical risk assessment tools for fatiguing lifting tasks has not been explored yet. For instance, myoelectric manifestations of muscle fatigue can be estimated using bipolar sEMG by monitoring changes in the amplitude and frequency of the signals over time (Cifrek et al., 2009; Merletti and Parker, 2004; Merletti and Farina, 2016) attributed to fatigue-induced changes in muscle fibers conduction velocity (Farina and Merletti, 2003; Farina and Merletti, 2004). On the other hand, high-density sEMG (HDsEMG) can be used to evaluate the spatial distribution of the muscle activity and to estimate the discharge times of motor units by using decomposition algorithms (Farina et al., 2016; Negro et al. 2016; Falla and Gallina; 2020). An important advantage of HDsEMG over traditional bipolar sEMG, is the improved spatial sampling attributed to the multi-channels grids, which cover a wider muscle region than that of single pairs of electrodes (Del Vecchio et al., 2020; Madeleine et al., 2006; Farina et al. 2008; Gallina and Botter, 2013; Falla et al., 2017, 2014). A wider spatial sampling allows assessment of the changes in the distribution of muscle activity during various motor tasks (Farina et al., 2008; Falla and Farina, 2008; Tucker et al., 2009). Redistribution of muscle activity during sustained or repetitive tasks appears to have the physiological and functional significance of minimizing muscle fatigue whilst and maintaining motor output (Falla and Gallina, 2020; Farina et al., 2008; Gallina and Botter, 2013; Falla et al., 2014). Redistribution of muscle activity was particularly evident for the lumbar erector spinae, where a correlation was observed between endurance time and the extent of redistribution of erector spinae activity (Sanderson et al., 2019).

For these reasons and given of the better spatial sampling provided by HDsEMG compared to bipolar sEMG, in this study we aimed to verify the hypothesis that the combined use of HDsEMG and segmental kinematic assessment allows an optimized discrimination of risk levels associated with different fatigue lifting conditions.

2. Materials and Methods

2.1 Participants

Fifteen asymptomatic participants (9 female; age: 27.87±3.98 years; body mass index [BMI]: 25.26±3.21 kg/m^2) were recruited according to the following inclusion criteria: participants must have the capacity to give informed written consent, no relevant history over the last three years of back or lower limb pain or injury that limited their function and/or required treatment from a health professional. Exclusion criteria were concurrent systemic, rheumatic or neuro-musculoskeletal disorders which may confound testing, current pregnancy, currently on high doses of opioids (> 30 mg of morphine equivalent dose).

All participants gave their informed written consent before taking part in the study, which was conducted according to the Declaration of Helsinki at the Centre of Precision Rehabilitation for Spinal Pain (CPR Spine), the University of Birmingham, approved by the School of Sport, Exercise & Rehabilitation Sciences Ethics Committee (protocol number MCR260319-1).

2.2 Experimental procedure

The participants performed lifting tasks in three different lifting conditions selected to obtain the Lifting Index (LI) values of 1, 2, and 3 (Waters et al., 1994). LI was calculated as the ratio between the actual weight of the lifted load (L) and the recommended weight limit (RWL). RWL provided an estimate of the level of physical demand associated with the lifting task (Waters et al., 1994) and was calculated according to the RNLE as:

$$RWL = m_{ref} x HM x VM x DM x AM x FM x CM \tag{1}$$

where m_{ref} is the reference mass for the identified user population group, HM, VM, DM and AM are the horizontal distance, vertical distance, vertical displacement and asymmetry multipliers calculated by using equations or derived by tables by measuring appropriate parameters (horizontal distance (H), vertical location (V), vertical travel displacement (D) and angle of asymmetry (A)), CM is the coupling multiplier for the quality of gripping and FM is the frequency multiplier depending on lifting frequency (F), lifting duration and vertical location. Table 1 shows, for each lifting condition, the values of L, H, V, D, A, F and the corresponding values of the multipliers HM, VM, DM, AM, FM and CM. The hand-to-object coupling was defined as "good" for all three lifting tasks (Waters et al., 1994). The three conditions differed only the values attributed to F and FM while remaining parameters and multiplies assumed the same values.

Task	**LC (kg)**	**H (cm)**	**HM**	**V (cm)**	**VM**	**D (cm)**	**DM**	**A (°)**	**AM**	**F (lift/min)**	**FM**	**C**	**CM**	**L (kg)**	**RWL**	**LI**
A	23	44	0,57	75	0.99	40	0.93	0	1	4	0.83	good	1	10	15	**1**
B	23	44	0,57	75	0.99	40	0.93	0	1	11	0.41	good	1	10	7.5	**2**
C	23	44	0,57	75	0.99	40	0.93	0	1	15	0.28	good	1	10	5	**3**

Table 1. For each task (A, B, and C), the values of the load weight (L), the horizontal (H) and vertical (V) locations, the vertical travel distance (D), the asymmetry angle (A), the lifting frequency (F) and the hand-to-

object coupling (C) and the corresponding values of the multipliers (HM, VM, DM, AM, FM, CM), the recommended weight limit (RWL) and the lifting index (LI).

Tasks were performed with the participant standing in a neutral body position with his/her feet parallel spaced at a natural standing distance for him/her. The task consisted of lifting a plastic crate (34x29x13 cm) with handles using both hands in the three different lifting conditions. The participants performed the lifting tasks in three different sessions performed on three different days, one for each LI. The different lifting sessions were randomly (selecting numbers between one and three from an opaque envelope) executed across the three days. The three sessions were 72 hours apart and conducted at the same time of the day for each participant to avoid confounding effects due to fatigue or daily habits (Filho et al., 2013). The duration of each of the lifting tasks was 15 minutes. The number of repetitions was determined by the frequency parameter used to obtain the specific LI of the session. A timer and acoustic feedback were used to monitor the duration of lifting and the frequency of tasks, respectively.

2.3 Electromyographic and kinematic recordings

2.3.1 Bipolar and HDsEMG

Muscle activity was acquired via two wireless bipolar sEMG sensors (Ultimium EMG system, Noraxon, USA Inc. Scottsdale, AZ) bilaterally from the erector spinae longissimus (ESL), following guidelines for electrode placement (seniam) and the atlas of muscle innervation zones (Barbero et al., 2012).

HDsEMG was acquired via two 64 channels grids placed 2.5 cm away from the spinous process, between the 2nd and 5th lumbar vertebra (see Fig. 1A) (Falla et al., 2014; Sanderson et al., 2019). The grid consisted of 13 rows and 5 columns of electrodes (1-mm diameter, 8-mm interelectrode distance in both directions), with one electrode absent from the upper right corner (Fig. 1A)). The position corresponding to the missing electrode was used as the origin of the coordinate system to define the electrode location. Prior to the application of electrodes, the skin in the region lateral to the lumbar spine was prepared by shaving the area if needed, applying an abrasive paste (SPES Medica, Italy), and finally washing and drying the region. The electrodes were prepared by applying a thin custom double-sided adhesive foam pad to the electrode grid (SPES Medica, Genoa, Italy) where the cavities of the electrode grids were filled with an electroconductive paste (SPES Medica). Reference electrodes were placed on prepared skin over the sacrum, posterior and anterior superior iliac spines. The EMG signals were amplified (128-channel surface EMG amplifier, OT Bioelettronica; #3 dB bandwidth 10-500 Hz) by a factor of 2000 and sampled at 2048 Hz.

All devices were synchronized together during lifting tasks with a trigger signal generated by a synching device (MyoSync, Noraxon).

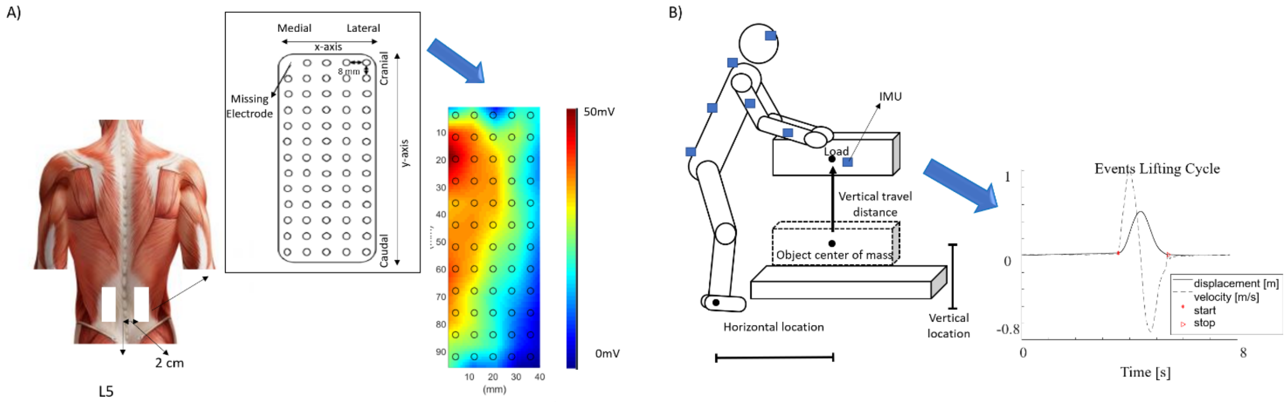

Fig. 1. Description of the experimental setup. A) Positioning of the HD-sEMG grids: 2.0 cm lateral to the L5 spinous process on the lumbar ES. Schematic representation of the electrode grids showing the x- and y-axes and inter-electrode distance (left) and an example of topographical maps (see the text for further details). B) On the left, setup and IMUs sensor configuration and the right, displacement and velocity of IMU placed on the load. These curves were used to define the lifting cycle: the events of lifting start and stop are also reported (see the 2.5.1 for further details).

2.3.2 Kinematic assessment

Inertial sensors (myoMotion Research PRO IMU, Noraxon) were used to acquire movements of the following body segments (Fig. 1B): the head (in the middle of the back of the head), upper thoracic (T2), lower thoracic (over the spine at L1/T12), pelvic (bony area of the sacrum at L5-S1 level), right arm (mid-length of the humerus) and right forearm (mid-length of the forearm). An additional IMU was placed on the plastic crate (z-axis in the vertical direction). Calibration was carried out with the participant in a standing upright position to determine the value of the 0° angle of the assessed body segments. Sampling frequency for the inertial sensors was set at 200 Hz.

2.4 Questionnaires data

At the end of each session, participants completed a visual analogue scale (VAS) which was used to rate pain intensity in the low back region (with 0-100 as anchor points for no pain and the worst pain imaginable, respectively) and the Borg scale to rate fatigue (with 6-20 as points for extremely light and extremely hard perceived exertion, respectively; (Borg, 1982)).

2.5 Data Analysis

Data were processed using Matlab (version 8.0.0.783; MathWorks, Natick, MA, USA) software. Kinematic, kinetic and electromyographic data during the lifting task were time-normalized to the duration of the lifting task. The data were interpolated to 100 samples for the lifting phase and 100 for the lowering phase: the interpolated value at a query point is based on linear interpolation of the values at neighbouring grid points in each respective dimension.

2.5.1 Lifting cycles detection

The vertical displacement and velocity of the IMU placed over the crate were calculated. To estimate vertical velocity and displacement, the filtered acceleration of IMU (3rd order low-pass Butterworth filtered by applying a 10Hz cut-off frequency) was integrated once and twice respectively, and the drift was corrected assuming that before and after lifting the vertical acceleration and speed were zero. The onset of the lifting task was defined as the time point at which the IMU velocity exceeded a velocity threshold of 0.025 m/s (Ranavolo et al., 2015) along the vertical axis. End of the lifting task was defined where the IMU load velocity fell below the velocity threshold in the opposite direction after reaching the minimum value (see Fig. 1B). After the cycles definition, a Dynamic Time Warping approach (Muscillo et al., 2007) was used to align the curves that were shifted (see Fig. 2) if wrong events were detected.

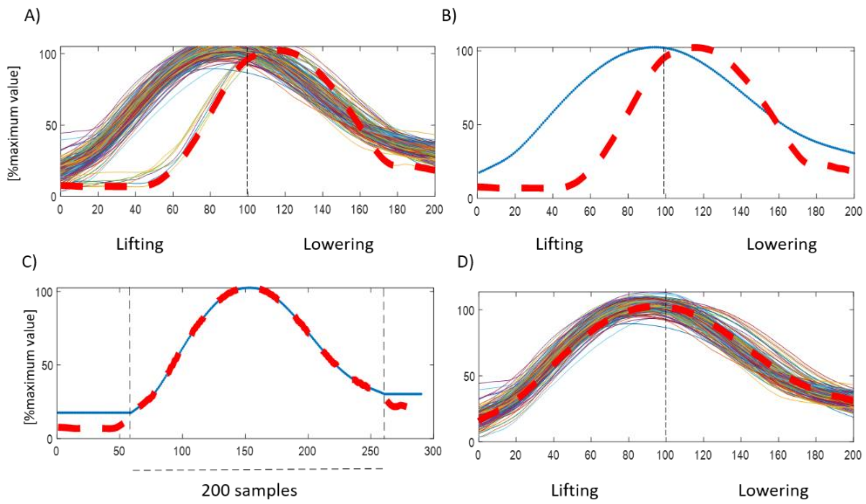

Fig. 2. Dynamic Time Warping (DTW) approach to align curves. A) Vertical displacement of the IMU placed over the load in all detected cycles; B) Mean curve and one shifted curve; C) Mean curve and aligned curve with DTW approach; D) Vertical displacement of the IMU placed over the load in all aligned cycles.

2.5.2 Bipolar sEMG

The sEMG signals for each lifting task were band-pass filtered using a 3rd-order Butterworth filter of 20–400 Hz to reduce low-frequency artifacts and high-frequency noise (Butler et al. 2009; Drake and Callaghan, 2006). To extract the envelope of sEMG signals of each lifting task, full-wave rectification, and low-pass filtering using a fourth-order Butterworth filter at 5 Hz were applied (Winter, 2009). Then, to highlight differences in the sEMG activity between different conditions, the root mean square (RMS) within the cycle was calculated. All the acquired data – all the conditions (LI=1, 2 and 3) of all the lifting tasks – were time-averaged over one-minute windows and expressed as a percentage relative to the initial value (first value of the task) (Falla et al., 2014).

2.5.3 HDsEMG

HDsEMG signals were digitally band-pass filtered in the frequency bandwidth 20–400 Hz (3rd order Butterworth filter). Fifty-nine bipolar EMG signals were obtained from each grid (12 longitudinal bipolar recordings in each column except the first column of the grid, which had 11 electrode pairs). To characterize the spatial distribution of muscle activity, the RMS values were computed from each of 59 bipolar recordings from adjacent, nonoverlapping signal epochs of 0.5-second duration, as described in Farina et al. (2008) and in Falla et al. (2014). The RMS values for each bipolar signal were used to create a topographical map of ESL activity. For graphical representation, the 59 values were interpolated by a factor of 8, but only the original values were used for data processing and statistical analysis. The individual RMS values for each bipolar signal were averaged to produce the mean RMS across the grid (RMS_{full_grid}). Furthermore, for each cycle, the region of activation (RoA) was determined as follows: the mean RMS for the area of each four neighbouring electrodes was determined, and the RoA was considered as the area with higher mean RMS (RMS_{RoA}, see Fig. 3).

For each condition (LI=1, 2 and 3) of all the lifting tasks, RMS_{full_grid} and RMS_{RoA} were time-averaged over one-minute windows and expressed as a percentage relative to the initial value (first value of the task) (Falla et al., 2014).

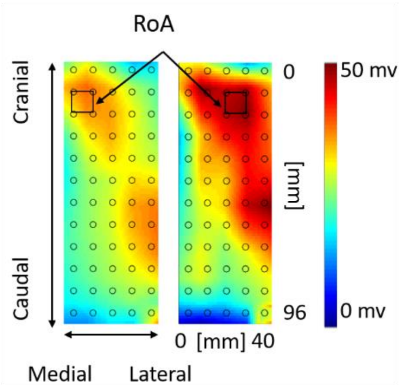

Fig. 3. Region of activation (RoA) definition.

2.5.4 Kinematics: Acceleration and Jerk

Stability parameters were evaluated from the acceleration signals: the RMS of the acceleration magnitude ($RMS_{acc\_magnitude}$) and the RMS of the jerk (i.e. the derivative of the acceleration) magnitude (RMS_{jerk}) (Fazio et al., 2013).

2.6 Statistical Analysis

All of the statistical analyses were performed using Matlab software (version 2018b 9.5.0.1178774, MathWorks, Natick, MA, USA). For each parameter (kinematic and sEMG), the normality of data distribution was checked using the Shapiro-Walk test. One-way repeated-measures analysis of variance (ANOVA) was performed to determine whether LI levels determine significant changes in each parameter. Post-hoc analyses were performed using a paired t-test with Bonferroni's corrections when significant differences were observed. Furthermore, for each lifting condition and EMG parameter, we applied a parametric paired-samples t-test to detect any differences between the right and left side. P values < 0.05 were considered statistically significant.

3. Results

3.1 Bipolar sEMG

Fig. 4 shows the mean envelopes (± Standard Deviation, SD) for each lifting condition of right and left ESL during the lifting (100 samples) and lowering cycles (100 samples).

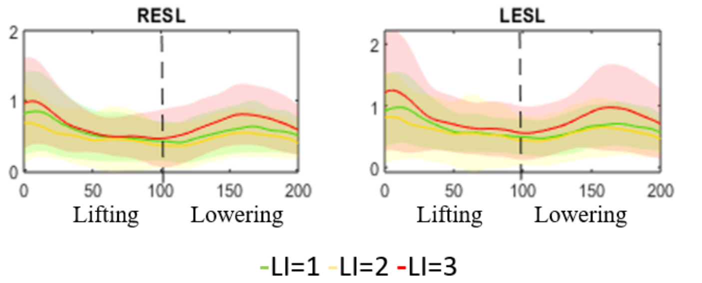

Fig. 4. Mean envelopes (± SD) for each lifting condition of the right (RESL) and left (LESL) erector spinae – longissimus during the lifting (100 samples) and lowering cycles (100 samples).

Since no statistically significant differences were found between sides ($p > 0.05$), the following results uniquely refer to the right side only.

Fig. 5A shows the mean and standard deviation values of RMS for each LI during each minute of the lifting cycles. For each considered epoch, one-way ANOVA showed significant effects for RMS considering LI ($p < 0.05$). The statistical significances for the post hoc analysis are reported in Fig. 5A.

3.2 HDsEMG

Since no statistically significant differences were found between sides for RMS_{full_grid} and RMS_{RoA} ($p > 0.05$), the following results uniquely refer to the right side.

The mean and standard deviation values of RMS_{full_grid} and RMS_{RoA} for each LI, during each minute of the lifting cycles, are reported in Fig. 5B and 5C. For each considered epoch, one-way ANOVA showed significant effects for both RMS_{full_grid} and RMS_{RoA} considering LI ($p < 0.05$). The statistical significance of post hoc analysis is reported in Fig. 5B and 5C.

Fig. 6 shows the topographical map of RESL EMG amplitude for a representative participant for LI=1 (A), LI=2 (B) and LI=3 (C) recorded at 2 min intervals throughout the task. In each map, the RoA is represented as a black square.

Fig. 7 shows the map of activation of RESL for a representative participant for LI=1 (A), LI=2 (B) and LI=3 (C) in a cycle of the 1st minute and a cycle of the 15th minute.

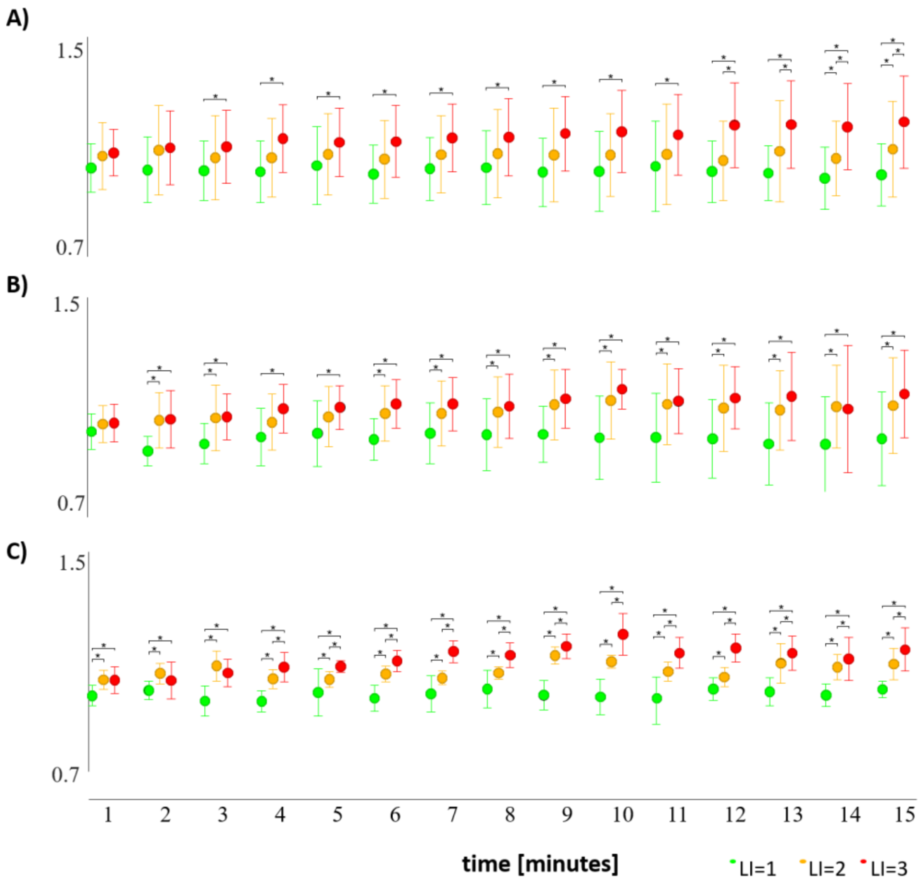

Fig. 5. Mean and standard deviation values of RMS of erector spinae longissimus (ESL) for bipolar signals (A), for all grid of HD signals (RoA_{full_grid}, B)) and of RoA of HD (RMS_{RoA}, C)) for each LI during lifting cycles. *statistical significance. RMS: root mean square; HD: high density; RoA: region of activation.

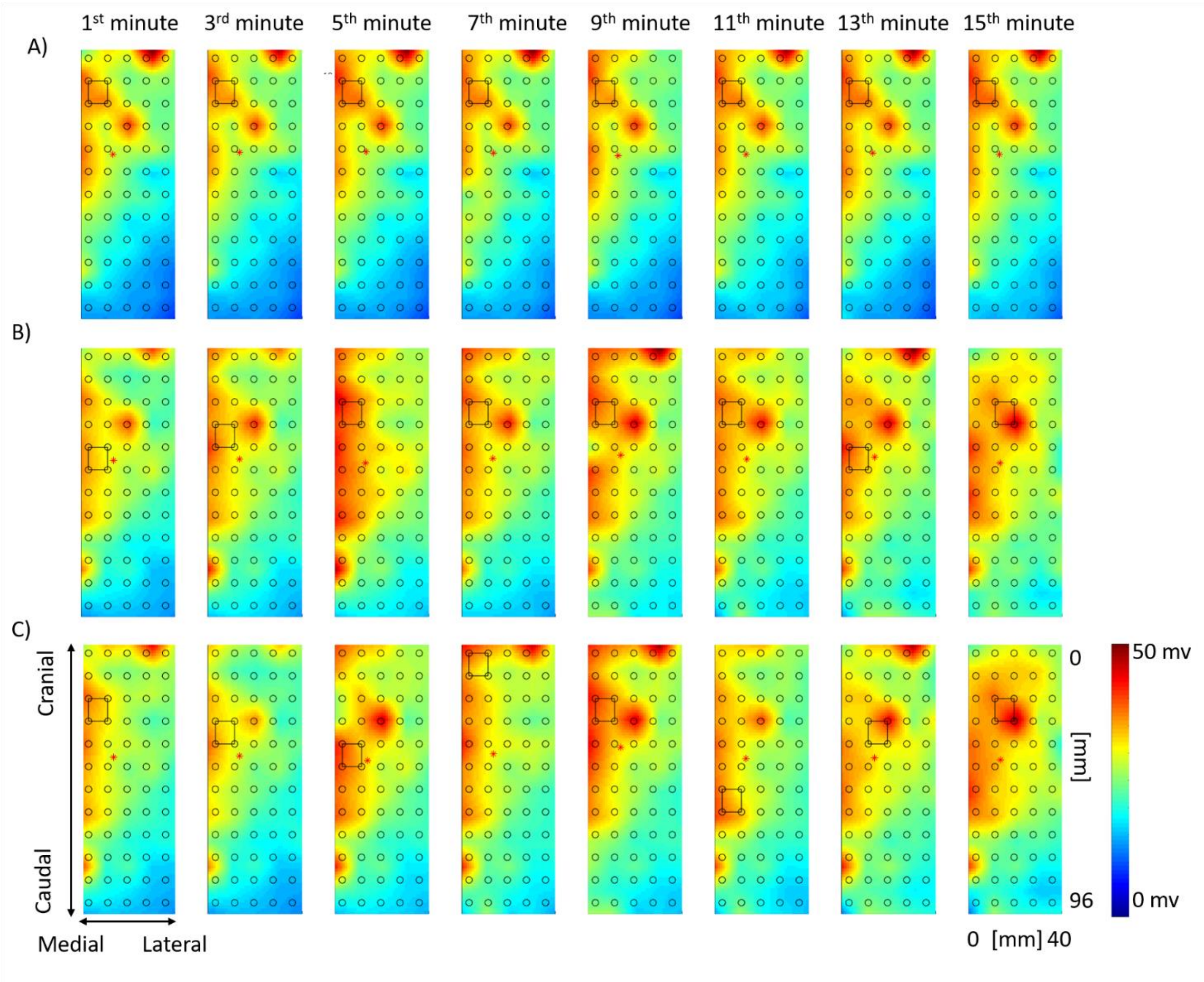

Fig. 6. Topographical EMG amplitude maps recorded from the right erector spinae – longissimus for a representative participant for LI=1 (A)), LI=2 (B)) and LI=3 (C)) from the first minute to the last minute of the task. The square is the region of activation (RoA).

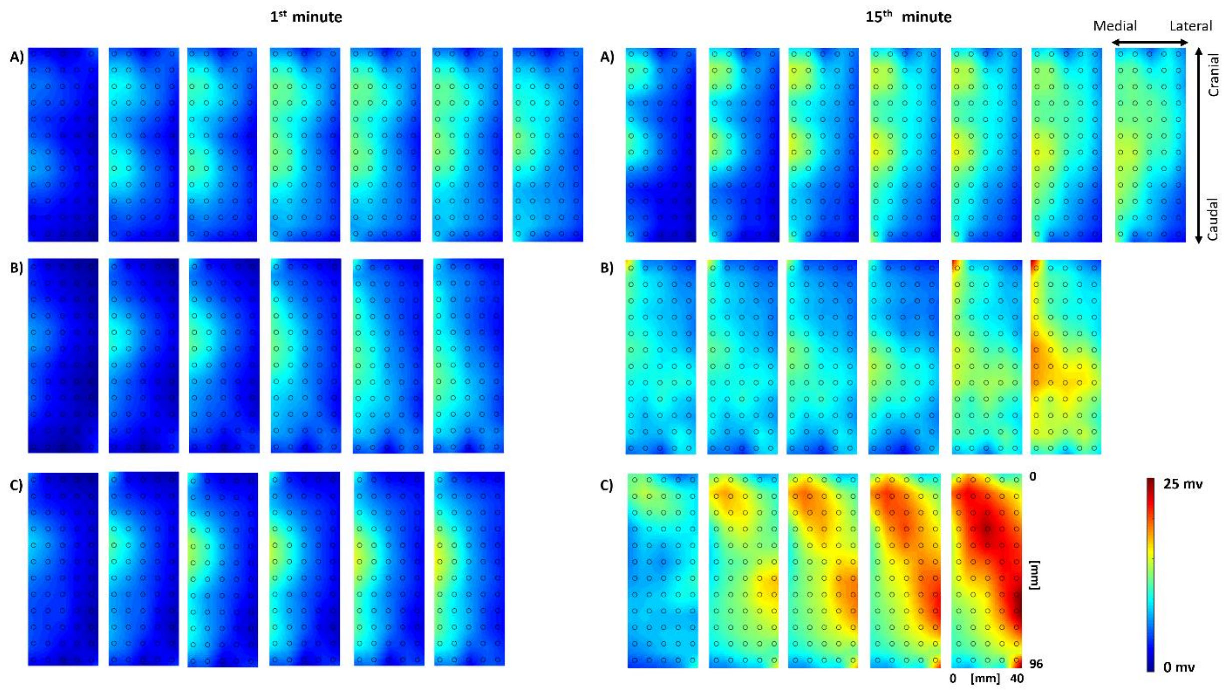

Fig. 7. Topographical EMG amplitude maps recorded from the right erector spinae – longissimus for a representative participant for LI=1 (A)), LI=2 (B)) and LI=3 (C)) in a cycle of the first minute and a cycle of the last minute of the task.

3.3 RMS of acceleration and jerk

Fig. 8 shows the mean and standard deviation values of $RMS_{acc\_magnitude}$ and RMS_{jerk} for each IMU and each LI during each minute of the lifting cycles. For each considered epoch, one-way ANOVA showed significant effects for both $RMS_{acc\_magnitude}$ and RMS_{jerk}, considering the LI ($p < 0.05$). The statistical significance of post hoc analysis is reported in Fig. 8.

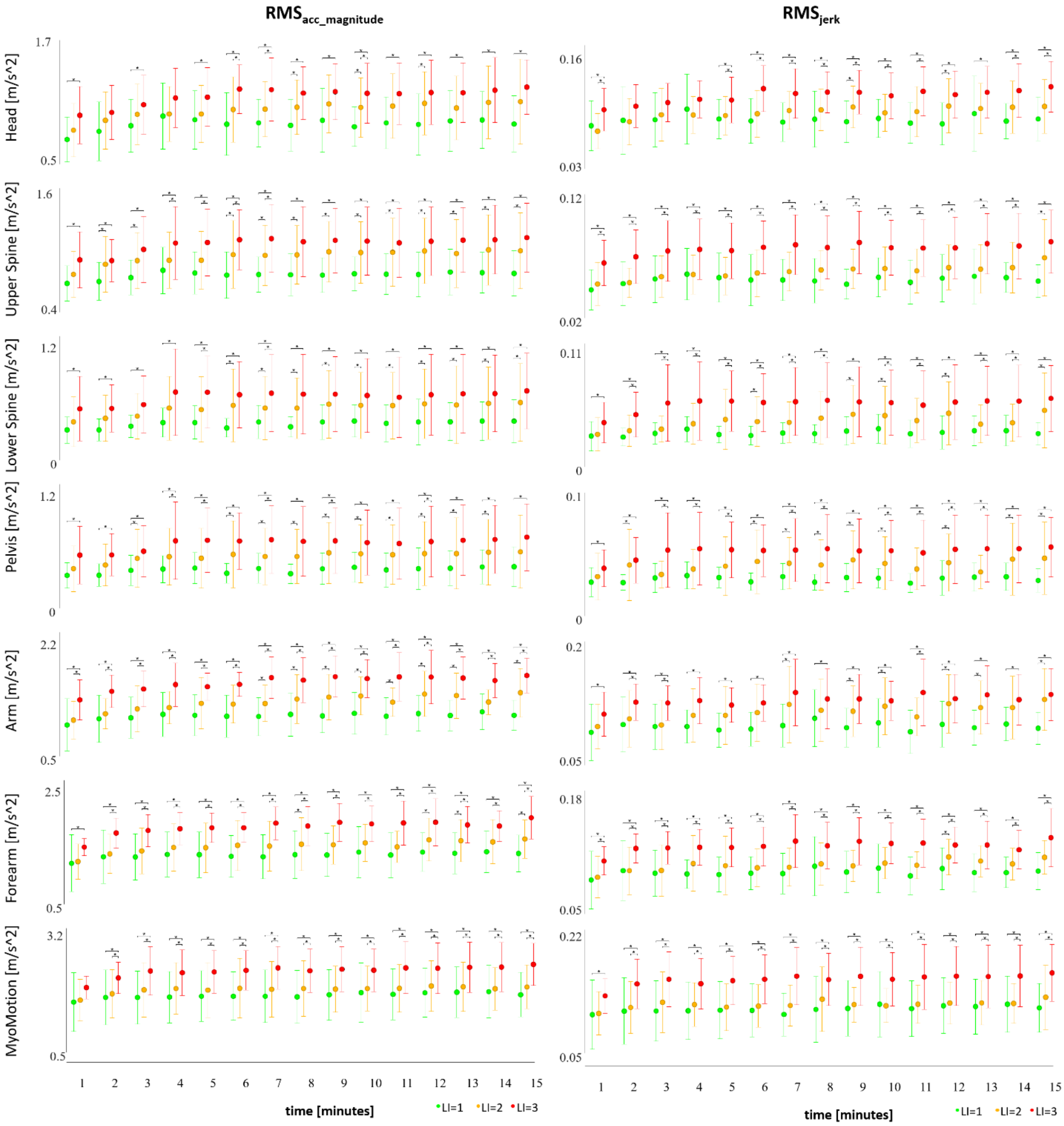

Fig. 8. Mean and standard deviation values of the RMS of the acceleration magnitude ($RMS_{acc\_magnitude}$) and the RMS of the jerk magnitude (RMS_{jerk}) for each IMU and each LI considering lifting cycles. *statistical significance. RMS: root mean square.

3.4 Questionnaires

The values of VAS and Borg scale at the end of each session are reported in **Table 2.** The repeated measures ANOVA revealed no significant effect of the LI on perceived pain (p=0.114) but a significant effect on perceived fatigue (p<0.001). Post hoc analysis showed significant differences between LI=1 and LI=2 for perceived fatigue ($p=0.04$) and between LI=1 and LI=3 for perceived fatigue ($p=0.002$).

Scale	LI	Mean±SD
VAS (0-100)	1	1.4±3.22
	2	4.73±10.81
	3	11.6±22.78
Borg Scale (6-20)	1	7.53±1.55
	2	9.2±2.62
	3	10.1±2.65

Table 2. Pain and fatigue scores measured at the end of each lifting task. VAS, visual analogue scale (0-100); LI, Lifting Index. Values are presented as mean ± SD.

4. Discussion

This study investigates, for the first time, the upper body kinematics using IMUs and erector spinae behaviour using both sEMG and HDsEMG approaches to detect three risk conditions related to fatiguing frequency-dependent lifting designed using the RNLE. Previous sensors-based investigations were limited to single frequency-independent lifting tasks by considering the frequency multipliers of RNLE equal to 1 and excluding the influence of muscle fatigue. Expanding the analysis capacity would allow better preventive strategies for handling heavy loads which occur in many workplaces (Le et al., 2017) and are considered one of the main causes of WLBDs. The risk of lifting-related WLBDs increases as the lifting frequency increases (Johanning, 2000). WLBDs account for 13-24% of all workplace injuries and illnesses, 15-25% of the annual number of sick leave days, 25% of workers' yearly compensation expenses (Garg et al., 2014) and the 19% of Work-related Musculoskeletal Disorders (WMSDs) (Moreira-Silva et al., 2020).

The erector spinae activity showed an increased activation at the beginning of both lifting and lowering phases with a decrease until the upright position was reached, and the load was released (Fig. 4). The results did not reveal any side to side difference of erector spinae activity for any of the lifting conditions, not even in the most demanding one where fatigue could perhaps give rise to asymmetric activation. Such finding provides relevant information for the future development of new sEMG-based risk assessment tools in symmetric tasks, where only unilateral measurements can be relevant.

The ANOVA showed that, every minute of the trial, the RMS of bipolar sEMG was significantly influenced by changes in LI (Fig. 5); the higher the risk, the greater the muscle activity. While at the beginning of the session, differences among the three risk conditions were not detected, from the third to the 11th minute lower and higher levels of risk (LI=1 vs LI=3) were significantly different. The medium-risk condition was well distinguished from the high-risk condition only towards the end of the session (12th and 13th minute) while all the three risk conditions could be discriminated only at the end of the task (14th and 15th minute).

When we consider the HDsEMG results, the mean RMS across the grid (RMS_{full_grid}) and the mean RMS in the region of activation (RMS_{ROA}) were both sensitive to all three levels of risk; the higher the risk, the more significant the increase of RMS (Fig. 5B and C). Specifically, the RMS_{full_grid} revealed differences between low and medium (LI=1 vs LI=2) and low and high (LI=1 vs LI=3) risk levels which were already evident from the 2nd minute (Fig. 5B). When the RMS_{ROA} was considered, the differences between low and medium (LI=1 vs LI=2) and low and high (LI=1 vs LI=3) risk levels were detected from the beginning of the task (Fig. 5C). Starting from the 4th minute, the RMS_{ROA} could discriminate between the three risk levels (Fig. 5C) as possibly due to the higher spatial sampling achieved by the measure RMS_{full_grid}.

The RoA changed with the level of risk; at the low level of risk (LI=1, Fig. 6A) the RMS_{RoA} was static, whereas during the medium level of risk (LI=2, Fig. 6B) it changed slowly and at the high level of risk (LI=3, Fig. 6C) the RoA was highly variable/dynamic. This could imply that during more demanding, fatiguing tasks, there is a redistribution of activity to minimize or delay muscle fatigue; a feature which cannot be detected with traditional bipolar sEMG.

Additionally, the topographical maps of EMG amplitude during a lifting cycle (Fig. 7) show that during the task at the low level of risk (LI=1, Fig. 7A) there are no differences in the spatial distribution of erector spinae activity between the beginning (1st minute) and the end (15th minute) of the task. Conversely, when the level of risk increases (LI=2 and LI=3, Fig. 7B and 7C), changes in the distribution of erector spinae activity can be observed between the beginning and the end of the session becoming even more evident in the high-risk condition (Fig. 7). As previously stated, changes in the distribution of muscle activity during either sustained or repetitive tasks are considered to be functionally relevant to maintain motor output (Farina et al., 2008; Sanderson et al., 2019) and potentially avoid overload of the same muscle fibers during prolonged activation. During the task at a high level of risk, the shift in the distribution of muscle activity was in the caudal direction or the erector spinae (Fig. 7C). This finding is consistent with previous studies reporting an increase in sEMG amplitude in the more caudal region of the lumbar erector spinae compared to the more cranial region following tasks that induced fatigue (Falla et al., 2014; Tucker et al., 2009; Sanderson et al., 2019; Brazier et al., 1992; Martinez-Valdes et al., 2019; van Dieen et al., 1993).

Collectively, our findings suggest that it is possible to detect the risk level when monitoring fatiguing lifting tasks by using HDsEMG tools. Therefore, ergonomists and health and safety practitioners could detect the risk level in order to verify the efficacy of an ergonomic intervention. This is relevant considering the Industry 4.0 scenario (Kapelner et al., 2020) within which a fast pattern recognition and classification of workers' movement intentions is needed to control human-robot collaboration technologies such as wearable robots (i.e. exoskeletons). Recent research has led to an improvement in measuring and classifying myoelectric signals for man-machine interfaces thanks to neuro-musculoskeletal models driven by neural information decomposed by HDsEMG (Da Xu et al., 2018; Kapelner et al., 2019). Moreover, early detection of fatigue could be used to provide visual, acoustic or vibrotactile stimuli to workers alerting of muscular fatigue (Ajoudani et al., 2014).

For the kinematic data, the RMS of the acceleration magnitude ($RMS_{acc\_magnitude}$) and the RMS of the jerk magnitude (RMS_{jerk}, Fig. 8) distinguished the low and high level of risk (LI=1 vs LI=3**)**. Furthermore, for some parameters, there were significant differences between LI=1 and LI=2 or/and LI=2 and LI=3 (see Fig. 8). In particular, a better distinction between LI was obtained for the $RMS_{acc\_magnitude}$ for the IMU on the arm and forearm since they were able to significantly discriminate each pair of LI.

This study has many strengths, including the combined analysis and features extraction from EMG and Kinematic data. A possible limitation of this study could be its application in the workplace as HDsEMG requires more time to set up compared to bipolar sEMG. Such limitation can be mitigated by adopting wireless HDsEMG technology (limiting the amount of acquired channel to e.g. 64 channels).

In conclusion, HDsEMG can be used to discriminate low, medium and high-risk conditions where the lifting frequency of the RNLE changes. Machine-learning techniques, such as ANNS, can be used in future studies to estimate the biomechanical risk analyzing HDsEMG-extracted features. This approach can lead to a reliable biomechanical risk classification system for lifting tasks. Future developments could include the use of sensorized garments (SOPHIA project) to simplify the application of HDsEMG. The findings of this study can be used to extend the possibilities offered by the currently available instrumental-based tools on risk classification in lifting tasks. Such tools have only been used to investigate single frequency-independent lifting tasks (single repetition of task) so far (Alberto et al., 2018; Ranavolo et al., 2017, 2018, 2015; Varrecchia et al., 2018, 2020).

Funding: The research presented in this article was carried out as part of the program BRIC 2016-ID10 funded by INAIL and as part of the SOPHIA project, which has received funding from the European Union's Horizon 2020 research and innovation programme under Grant Agreement No. 871237.

Acknowledgments: We are extremely grateful to Alsubaie Amal M (AXA1435@student.bham.ac.uk); Haouidji-Javaux Nadège (n.c.haouidji-javaux@bham.ac.uk); Jiménez-Grande David(DBJ893@student.bham.ac.uk) of Centre of Precision Rehabilitation for Spinal Pain (CPR Spine), School of Sport, Exercise and Rehabilitation Sciences, University of Birmingham, Edgbaston, B152TT, United Kingdom for their help with the experimental procedure.

Conflicts of Interest: "The authors declare no conflict of interest."

References

1. Waters, T.R.; Putz-Anderson, V.; Garg, A.; Fine, L.J. Revised NIOSH equation for the design and evaluation of manual lifting tasks. *Ergonomics* **1993**, *36 (7)*, 749-776.
2. Waters, T.R.; Putz-Anderson, V.; Garg, A. *Applications Manual for the Revised NIOSH Lifting Equation*; U.S. Department of Health and Human Services: Cincinnati, OH, USA, 1994.
3. Lavender, S.A.; Li, Y.C.; Natarajan, R.N.; Andersson, G.B. Does the asymmetry multiplier in the 1991 NIOSH lifting equation adequately control the biomechanical loading of the spine? *Ergonomics* **2009**, 52, 71–79.
4. Alberto, R.; Draicchio, F.; Varrecchia, T.; Silvetti, A.; Iavicoli, S. Wearable monitoring devices for biomechanical risk assessment at work: Current status and future challenges—A systematic review. Int. J. Environ. Res. Public Health **2018**, 15, 2001; Erratum in 2018, 15, 2569, doi:10.3390/ijerph15112569.
5. Ranavolo, A.; Varrecchia T, Rinaldi M, Silvetti A, Serrao M, Conforto S, Draicchio F. Mechanical lifting energy consumption in work activities designed by means of the "revised NIOSH lifting equation". *Ind Health* **2017**, *55* (5), 444-454.
6. Ranavolo, A.; Varrecchia, T.; Iavicoli, S.; Marchesi, A.; Rinaldi, M.; Serrao, M.; Conforto, S.; Cesarelli, M.; Draicchio, F. Surface electromyography for risk assessment in work activities designed using the "revised NIOSH lifting equation". *Int. J. Ind. Ergon.* **2018a**, *68*, 34–45.
7. Ranavolo, A.; Mari, S.; Conte, C.; Serrao, M.; Silvetti, A.; Iavicoli, S.; Draicchio, F. A new muscle co-activation index for biomechanical load evaluation in work activities. *Ergonomics* **2015**, *58 (6)*, 966-979.
8. Varrecchia, T.; De Marchis, C.; Rinaldi, M.; Draicchio, F.; Serrao, M.; Schmid, M.; Conforto, S.; Ranavolo, A. Lifting activity assessment using surface electromyographic features and neural networks. *Int. J. Ind. Ergon.* **2018**, *66*, 1–9.
9. Varrecchia, T.; De Marchis, C.; Draicchio, F.; Schmid, M.; Conforto, S.; Ranavolo, A. Lifting activity assessment using kinematic features and neural networks. *Appl. Sci.* **2020**, *10*, 1989. Available online: https://doi.org/10.3390/app10061989 (accessed on 15 September 2020).
10. Cifrek, M.; Medved, V.; Tonković, S.; Ostojić, S. Surface EMG based muscle fatigue evaluation in biomechanics. Clin Biomech (Bristol, Avon). **2009**, *24(4)*, 327-340.
11. Merletti, R., Parker, P. Electromyography – Physiology, Engineering and Noninvasive Applications, first ed. John Wiley & Sons, Inc., Hoboken, New Jersey. **2004**.
12. Merletti, R; Farina, D. Surface Electromyography: Physiology, Engineering and Applications. Wiley–Blackwell. **2016.**
13. Farina, D.; Merletti, R. A novel approach for estimating muscle fiber conduction velocity by spatial and temporal filtering of surface EMG signals. *IEEE Trans Biomed Eng.* **2003**, *50 (12)*, 1340–1351.
14. Farina, D.; Merletti, R. Methods for estimating muscle fibre conduction velocity from surface electromyographic signals. *Med Biol Eng Comput*. **2004**, *42(4)*, 432–445. Review. Erratum in: Med Biol Eng Comput. 2004; 42(5):732.
15. Farina, D.; Negro, F.; Muceli, S.; Enoka, R.M. Principles of Motor Unit Physiology Evolve With Advances in Technology. Physiology (Bethesda). **2016**, *31(2)*, 83-94.
16. Negro, F.; Muceli, S.; Castronovo, A.M.; Holobar, A.; Farina, D. Multi-channel intramuscular and surface EMG decomposition by convolutive blind source separation. *J Neural Eng.* **2016**, *13 (2)*, 026027. doi:10.1088/1741-2560/13/2/026027.
17. Falla, D.; Gallina, A. New insights into pain-related changes in muscle activation revealed by high-density surface electromyography. *J Electromyogr Kinesiol.* **2020**; *52*, 102422. doi:10.1016/j.jelekin.2020.102422.
18. Del Vecchio, A.; Holobar, A.; Falla, D.; Felici, F.; Enoka, R.M.; Farina, D. Tutorial: Analysis of motor unit discharge characteristics from high-density surface EMG signals. *J Electromyogr Kinesiol.* **2020**, *53*, 102426.
19. Madeleine, P.; Leclerc, F.; Arendt-Nielsen, L.; Ravier, P.; Farina, D. Experimental muscle pain changes the spatial distribution of upper trapezius muscle activity during sustained contraction. *Clin Neurophysiol*, **2006**, *117 (11)*, 2436-45.
20. Farina, D.; Leclerc, F.; Arendt-Nielsen, L.; Buttelli, O.; Madeleine, P. The change in spatial distribution of upper trapezius muscle activity is correlated to contraction duration. *J Electromyogr Kinesiol*, **2008**, *18(1)*, 16–25.
21. Gallina, A.; Botter, A. Spatial localization of electromyographic amplitude distributions associated to the activation of dorsal forearm muscles. *Front Physiol.* **2013,** *4*, 367. doi: 10.3389/fphys.2013.00367.

22. Falla, D.; Cescon, C.; Lindstroem, R.; Barbero M. Muscle pain induces a shift of the spatial distribution of upper trapezius muscle activity during a repetitive task: a mechanism for perpetuation of pain with repetitive activity? *Clin J Pain* **2017**, *33,* 1006–1013.
23. Falla, D.; Gizzi, L.; Tschapek, M.; Erlenwein, J.; Petzke, F. Reduced task-induced variations in the distribution of activity across back muscle regions in individuals with low back pain. *Pain* **2014**, *155,* 944–953.
24. Falla, D.; Farina, D. Non-uniform adaptation of motor unit discharge rates during sustained static contraction of the upper trapezius muscle. *Exp Brain Res* **2008**, *191*, 363–370.
25. Tucker, K.; Falla, D.; Graven-Nielsen, T.; Farina, D. Electromyographic mapping of the erector spinae muscle with varying load and during sustained contraction. *J Electromyogr Kinesiol*. **2009**, *19(3)*, 373-379. doi:10.1016/j.jelekin.2007.10.003
26. Sanderson, A.; Martinez-Valdes, E.; Heneghan, N.R.; Murillo, C.; Rushton, A.; Falla, D. Variation in the spatial distribution of erector spinae activity during a lumbar endurance task in people with low back pain. *J Anat.* **2019**. doi:10.1111/joa.12935.
27. Filho, J.C.; Gobbi, L.T.; Gurjão, A.L.; Gonçalves, R.; Prado, A.K.; Gobbi, S. Effect of different rest intervals, between sets, on muscle performance during leg press exercise, in trained older women. *J Sports Sci Med.* **2013**; *12(1)*, 138-43. PMID: 24149737; PMCID: PMC3761766.
28. Seniam. Available online: www.seniam.org (accessed on 09 October 2020).
29. Barbero, M., Merletti, R., Rainoldi, A. Atlas of Muscle Innervation Zones: Understanding Surface Electromyography and its Applications. Springer, New York. **2012**. http://doi:10.1007/978-88-470-2463-2
30. Borg, G.A. Psychophysical bases of perceived exertion. *Med Sci Sports Exerc*. **1982**, *14*, 377–381
31. Muscillo, R.; Conforto, S.; Schmid, M.; Caselli, P.; D'Alessio, T. Classification of motor activities through derivative dynamic time warping applied on accelerometer data. *Conf Proc IEEE Eng Med Biol Soc.*, **2007**, 4930-4933.
32. Butler, H.L.; Newell, R.; Hubley-Kozey, C.L.; Kozey, J.W. The Interpretation of Abdominal Wall Muscle Recruitment Strategies Change when the Electrocardiogram (ECG) is Removed from the Electromyogram (EMG). *J Electromyogr Kinesiol.* **2009**, *19(2)*, 102–113. http://doi:10.1016/j.jelekin.2007.10.004.
33. Drake, J.D.; Callaghan, J.P. Elimination of electrocardiogram contamination from electromyogram signals: An evaluation of currently used removal techniques. *J Electromyogr Kinesiol*. **2006** *16 (2)*, 175-187.
34. Winter, D.A. Biomechanics and Motor Control of Human Movement, fourth ed. John Wiley & Sons, Inc, University of Waterloo, Waterloo, Ontario, Canada. **2009**.
35. Fazio, P.; Granieri, G.; Casetta, I.; Cesnik, E.; Mazzacane, S.; Caliandro, P.; Pedrielli, F.; Granieri, E. Gait measures with a triaxial accelerometer among patients with neurological impairment. *J. Neurol. Sci.*, **2013** *34*, 4, 435-440.
36. Le, P.; Aurand, A.; Dufour, J.S.; Knapik, G.G.; Best, T.M.; Khan, S.N.; Mendel, E.; Marras, W.S. Development and testing of a moment-based coactivation index to assess complex dynamic tasks for the lumbar spine. *Clin. Biomech.* **2017**, *46*, 23–32.
37. Johanning, E. Evaluation and management of occupational low back disorders. Am J Ind Med. 2000 Jan; *37(1)*, 94-111. doi: 10.1002/(sici)1097-0274(200001)37.
38. Garg, A.; Boda, S.; Hegmann, K.T.; Moore, J.S.; Kapellusch, J.M.; Bhoyar, P.; Thiese, M.S.; Merryweather, A.; Deckow-Schaefer, G.; Bloswick, D.; Malloy, E.J. The NIOSH lifting equation and low-back pain, Part 1: Association with low-back pain in the backworks prospective cohort study. *Hum. Factors* **2014**, *56*, 6–28.
39. Moreira-Silva, I.; Azevedo, J.; Rodrigues, S.; Seixas, A.; Jorge, M. Predicting musculoskeletal symptoms in workers of a manufacturing company. *Int. J. Occup. Saf. Ergon.* **2020**, *19*, 1–9.
40. Brazier, J.E.; Harper, R.; Jones, N.M.; O'Cathain, A.; Thomas, K.J.; Usherwood, T.; Westlake, L. Validating the SF-36 health survey questionnaire: new outcome measure for primary care. *BMJ,* **1992.** *305(6846)*, 160-164.
41. Martinez-Valdes, E.; Wilson, F.; Fleming, N.; McDonnell, S.J.; Horgan, A.; Falla, D. Rowers with a recent history of low back pain engage different regions of the lumbar erector spinae during rowing. *J Sci Med Sport.* **2019**, *22(11)*, 1206-1212. doi:10.1016/j.jsams.2019.07.007
42. van Dieen, J.H.; Toussaint, H.M.; Thissen, C.; van de Ven A. Spectral analysis of erector spinae EMG during intermittent isometric fatiguing exercise. *Ergonomics* **1993**, *36*, 407–414.
43. Kapelner, T.; Sartori, M.; Negro, F., Farina, D. Neuro-Musculoskeletal Mapping for Man-Machine *Interfacing. Sci Rep.* **2020**, *10*, 5834.

44. Da Xu, L.; Xu, E.L.; Li, L. Industry 4.0: State of the art and future trends. *Int. J. Prod. Res.* **2018**, 56, 2941–2962.
45. Kapelner, T.; Vujaklija, I.; Jiang, N.; Negro, F.; Aszmann, O.C.; Principe, J.; Farina, D. Predicting wrist kinematics from motor unit discharge timings for the control of active prosthese. *J Neuroeng Rehabil*. **2019**; *16*, 47.
46. Ajoudani, A., Godfrey, S.B., Bianchi, M., Catalano, M.G., Grioli, G., Tsagarakis, N., Bicchi, A. Exploring teleimpedance and tactile feedback for intuitive control of the pisa/iit softhand. *IEEE Trans. Haptics* 2014.
47. Sophia project. Available online: www.project-sophia.eu (accessed on 09 October 2020).

Figure 1

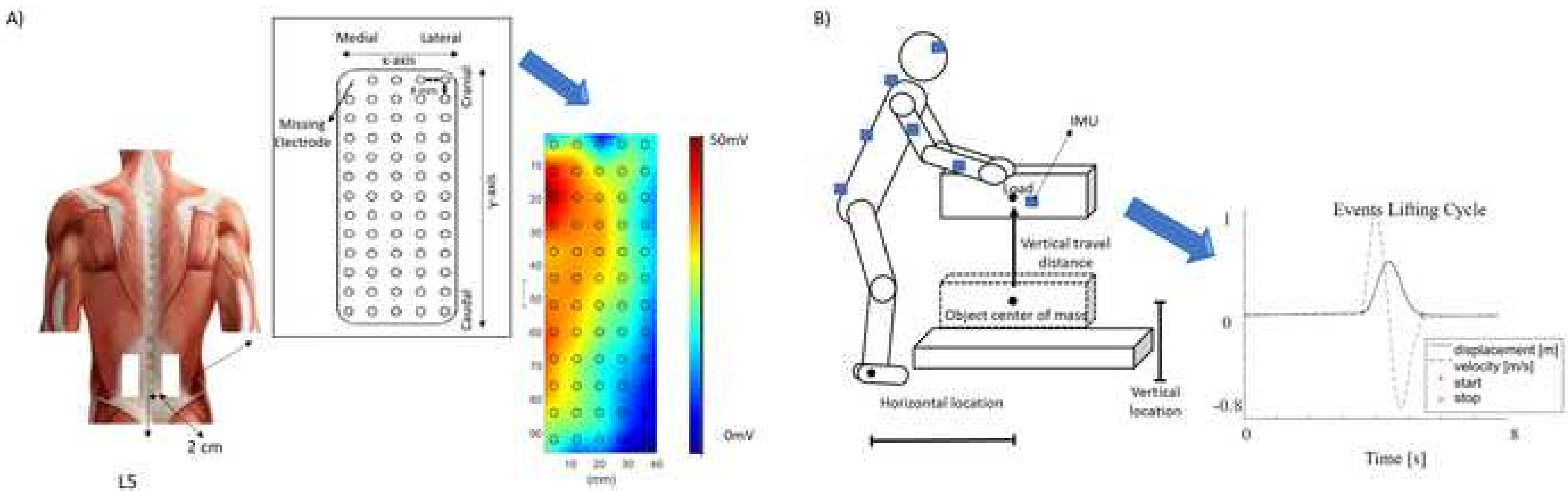

A)
Medial
Lateral
x-axis
Cranial
Caudal
y-axis
Missing Electrode
2 cm
L5
50mV
0mV
(mm)
B)
IMU
Load
Vertical travel distance
Object center of mass
Horizontal location
Vertical location
Events Lifting Cycle
displacement [m]
velocity [m/s]
start
stop
Time [s]

Figure 2

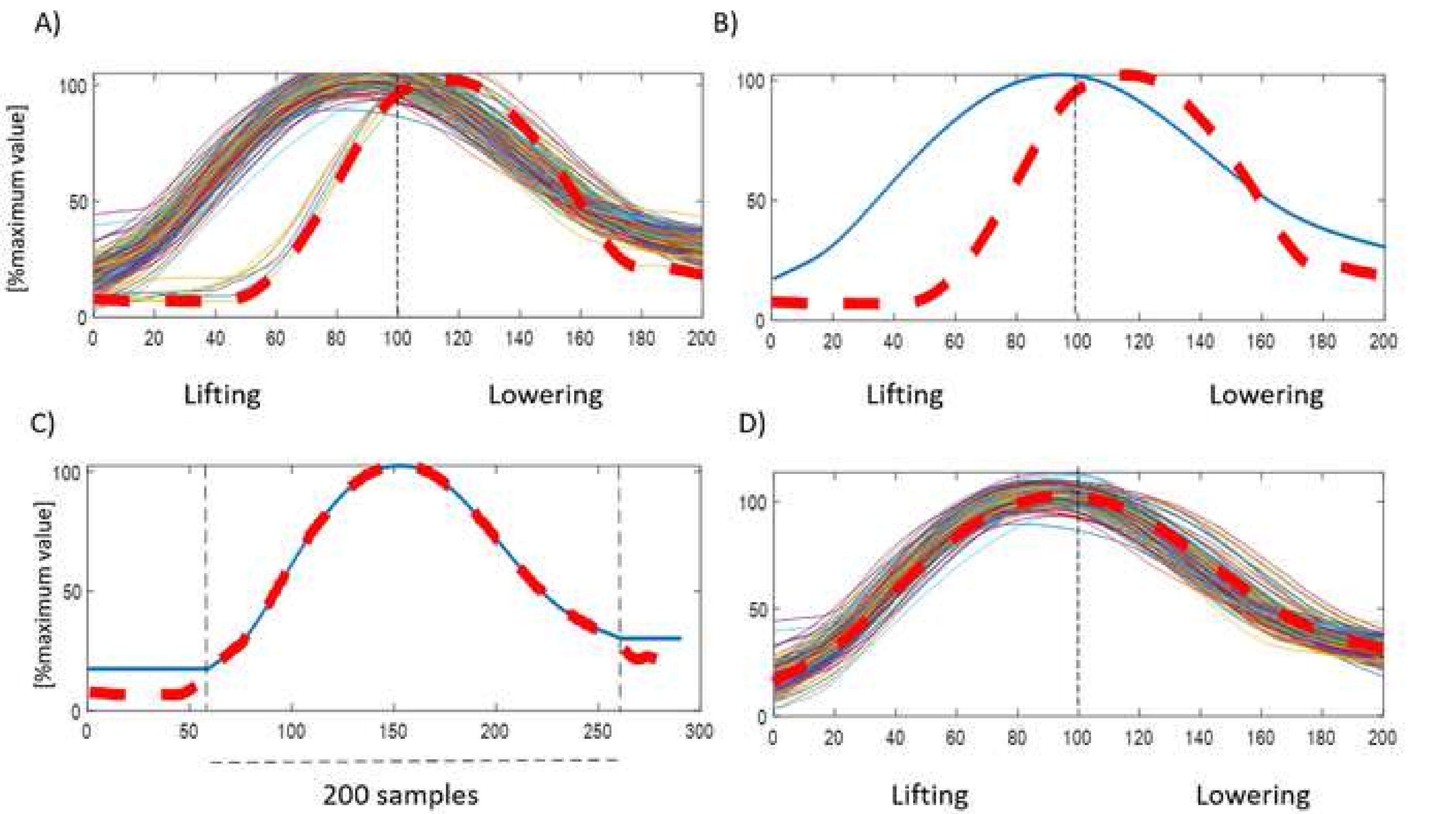
A)
B)
C)
D)
[%maximum value]
[%maximum value]
0
50
100
0
20
40
60
80
100
120
140
160
180
200
0
50
100
150
200
250
300
Lifting
Lowering
Lifting
Lowering
Lifting
Lowering
200 samples

Figure 3

Click here to access/download;Figure;Fig. 3.tif

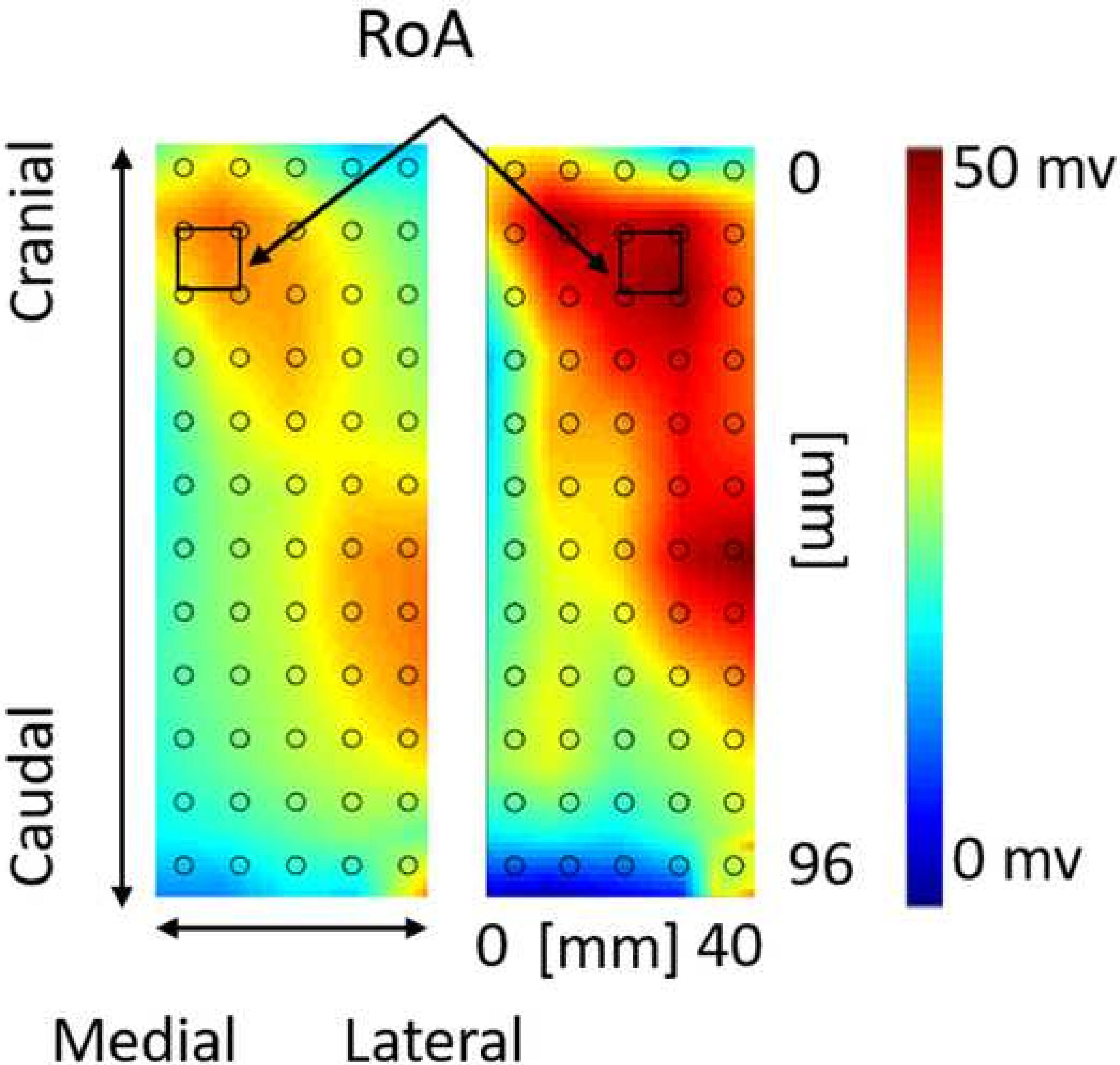

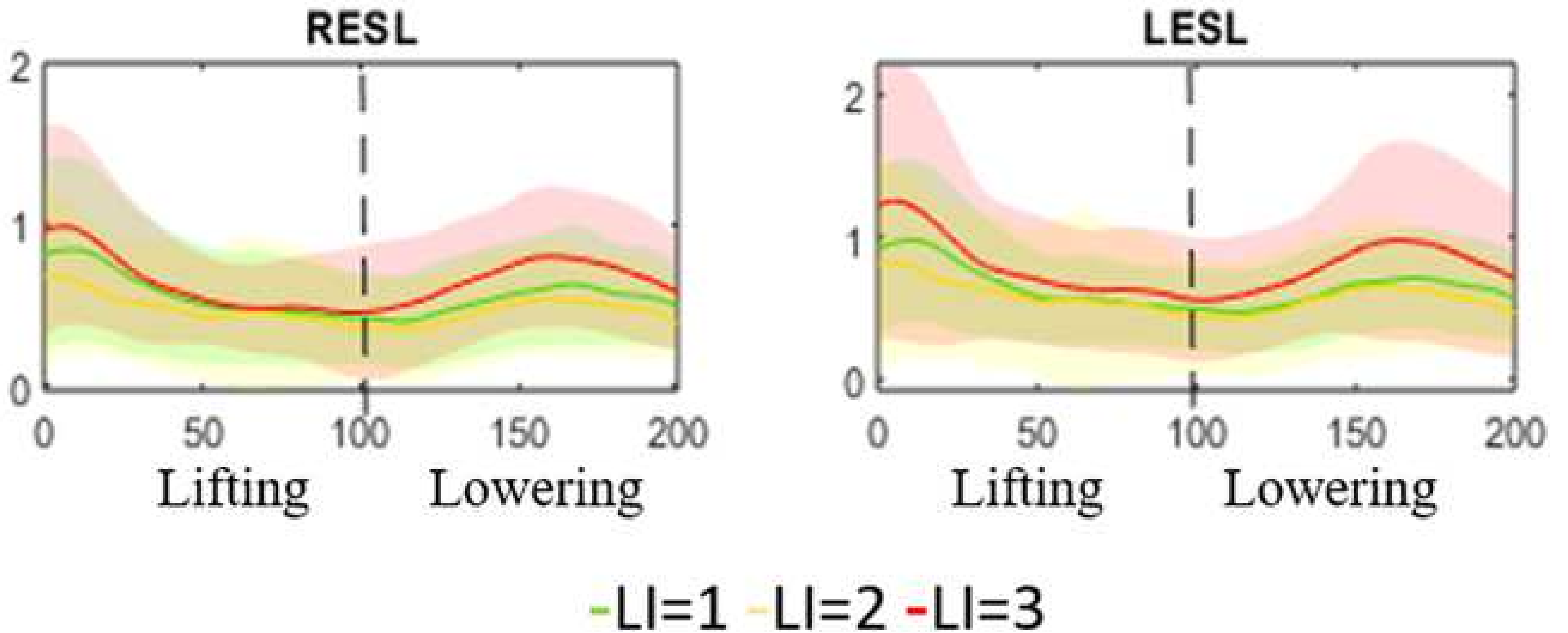
RESL
LESL
2
1
0
0
50
100
150
200
Lifting
Lowering
-LI=1 -LI=2 -LI=3

Figure 5

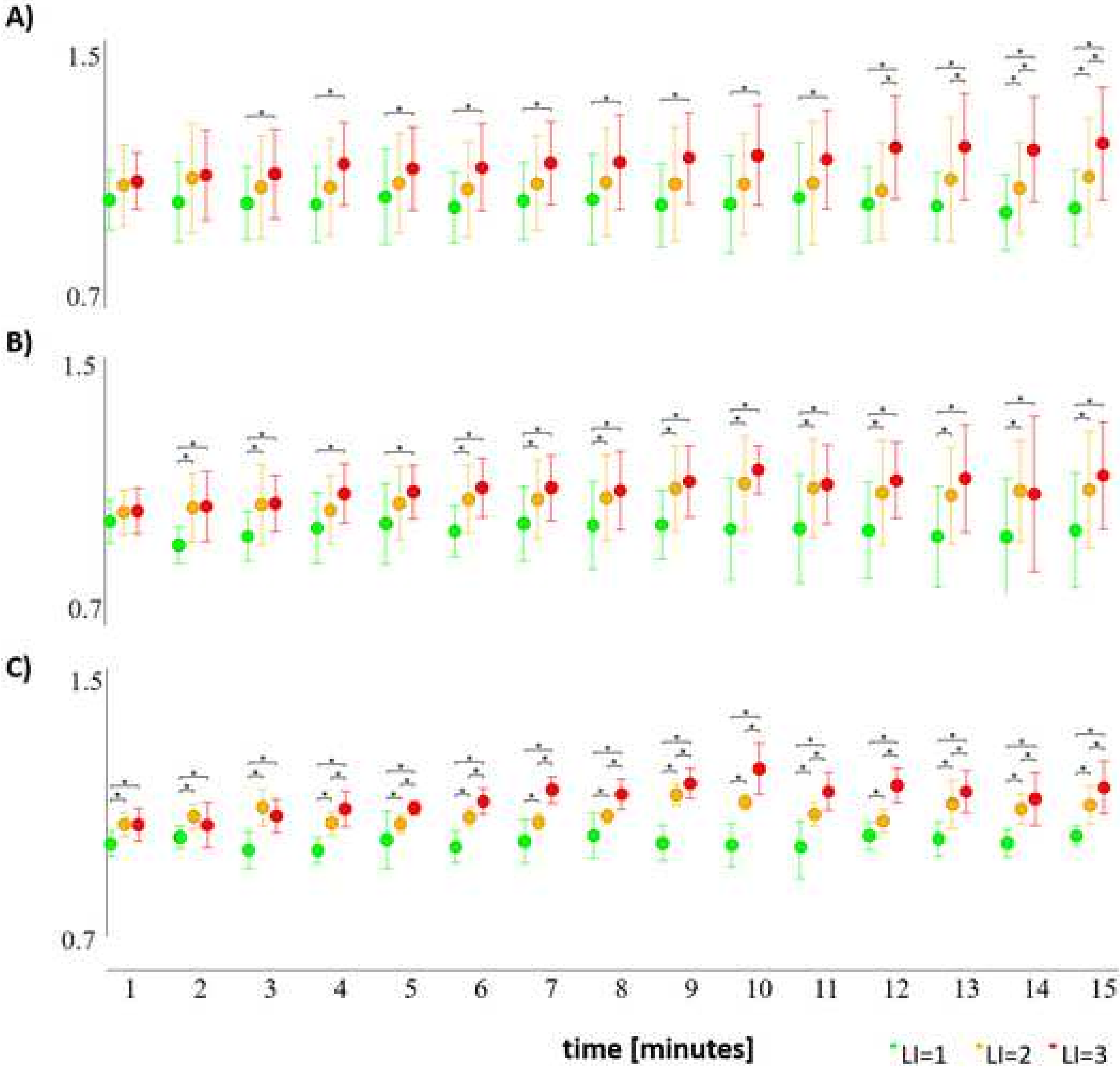

A)
1.5
0.7
B)
1.5
0.7
C)
1.5
0.7
1
2
3
4
5
6
7
8
9
10
11
12
13
14
15
time [minutes]
LI=1
LI=2
LI=3

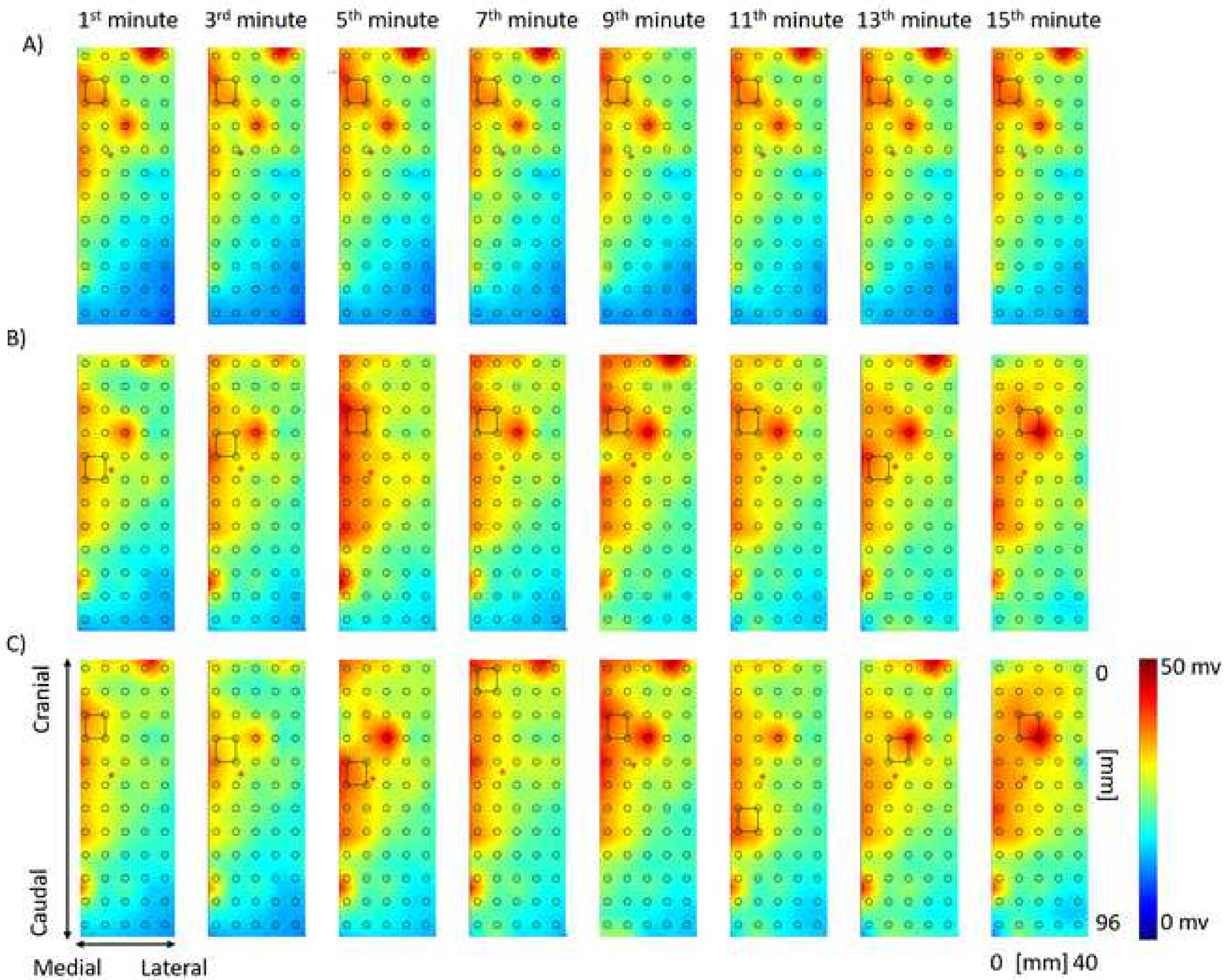

1st minute
3rd minute
5th minute
7th minute
9th minute
11th minute
13th minute
15th minute
A)
B)
C)
Cranial
Caudal
Medial
Lateral
0
[mm]
96
0 [mm] 40
50 mv
0 mv

Figure 7

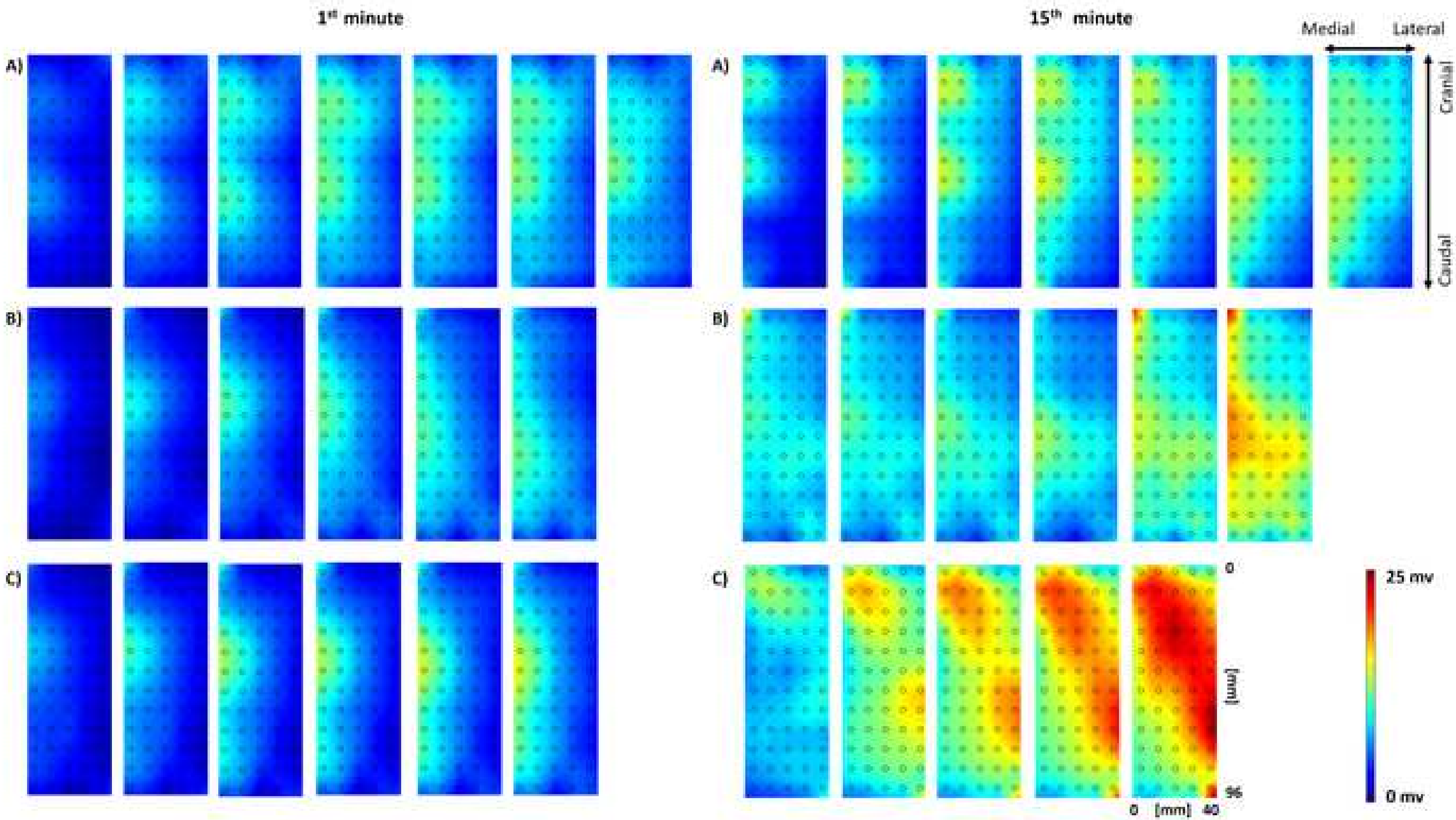
1st minute
15th minute
Medial
Lateral
Cranial
Caudal
A)
B)
C)
A)
B)
C)
0
[mm]
96
0 [mm] 40
25 mv
0 mv

Figure 8

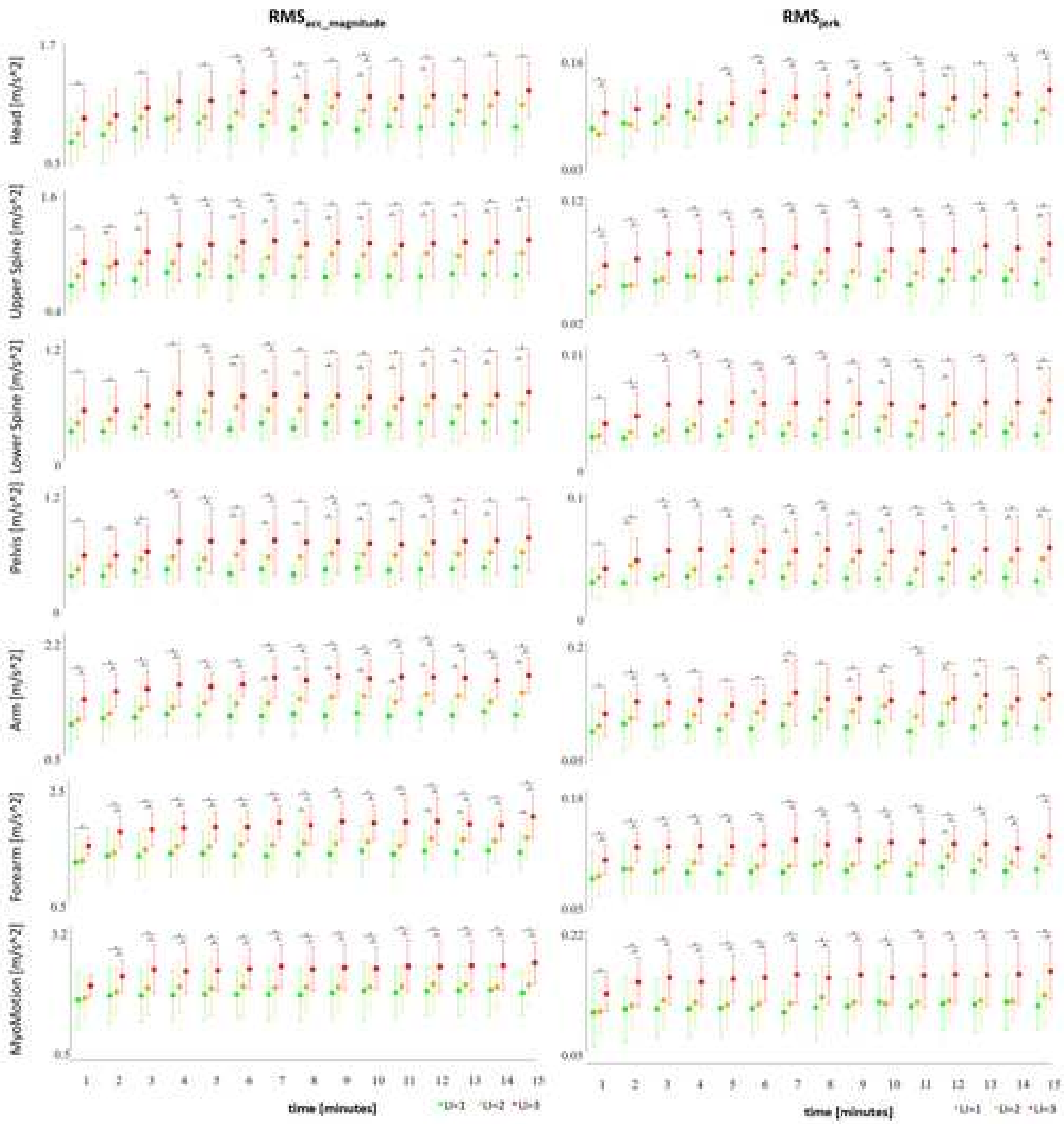
RMS acc_magnitude
RMS jerk
Head [m/s^2]
Upper Spine [m/s^2]
Lower Spine [m/s^2]
Pelvis [m/s^2]
Arm [m/s^2]
Forearm [m/s^2]
MyoMotion [m/s^2]
time [minutes]
LI=1
LI=2
LI=3

Declaration of interests

☒ The authors declare that they have no known competing financial interests or personal relationships that could have appeared to influence the work reported in this paper.

☐The authors declare the following financial interests/personal relationships which may be considered as potential competing interests: